

Control of Photovoltaic Grid Connected Using Different Control Strategies

Mostafa Bakkar

Dept. of Electrical and Control
Engineering
AAST
Alexandria, Egypt
mos_bico@yahoo.com

Mostafa Abd_El-Geliel

Dept. of Electrical and Control
Engineering
AAST
Alexandria, Egypt
maelgeliel@yahoo.com

Mahmoud Abo zied

Dept. of Electrical and Control
Engineering
AAST
Alexandria, Egypt
mca2ao@gmail.com

Abstract - A control method for two-stage utility grid-connected photovoltaic power conditioning systems (PCS) is proposed. This approach enables maximum power point tracking (MPPT) control with post-stage inverter current information instead of calculating solar array power although no information is needed on PV array, which significantly simplifies the controller and the sensing part.

In addition fuzzy logic control (FLC) method is presented and show difference between this method and other methods to control the PV power. In addition a combination of FLC with PCS is tested. MPPT using FLC has advantages of better performance, robust and simple design. In addition, this technique does not require the knowledge of the exact model of system and it can handle the nonlinearity. Modelling, controller design, simulation study of a grid connected PV system, and the overall configuration of the grid connected PV system is present.

Key words - photovoltaic (PV), maximum power point tracking (MPPT), Module Integrated Converter (MIC), PV power conditioning systems (PCS), proportional resonance (PR).

I. INTRODUCTION

PV power supplied to the utility grid is getting more and more visibility, while the world's power demand is increasing. Global demand for electrical energy is constantly growing. Along with the declining production of the dominating energy supplies since the industrial revolution, fossil fuels, there has been a growing interest in exploring renewable energies internationally [1]. Among a variety of the renewable energy sources, PV sources have no supply limitations and are predicted to become the biggest contributors to electricity generation among all renewable energy candidates by 2040 [2]. There are two topologies used to connect the PV with the grid: two stages and single stage PV system. A two stage is the traditional type and consists of a dc/dc converter direct coupled with PV array and a grid connected inverter. In single stage PV system the dc/ac inverter has more complex control goals; MPPT and output current control. Regardless its control complicity, single stage PV system is more efficient and cheaper than two stages system [3].

In this work, it was selected the two-stage PV energy conversion system, because it offers an additional degree of freedom in the operation of the system when compared with the one-stage configuration. Therefore, by including a dc-dc converter between the PV array and the inverter connected to the electric grid, various control objectives are possible to track concurrently with the PV system operation.

Since the generated power of PV system varies according to environmental condition, it is necessary to operate the PV at maximum power condition by using MMPT techniques. Many MPPT techniques have been scattered in literature. MPPT based on PCS is introduced. The introduced technique is compared with one of the conventional method and Fuzzy method. Moreover, a combination between Fuzzy and PCS technique is discussed.

II. PV SYSTEM CONFIGURATION

The single phase multi stage grid connected system being modelled is shown in Fig. 1. It consists of a PV array followed by step up stage feeding a current controlled voltage source inverter that feeds current into the single phase grid and local single phase loads.

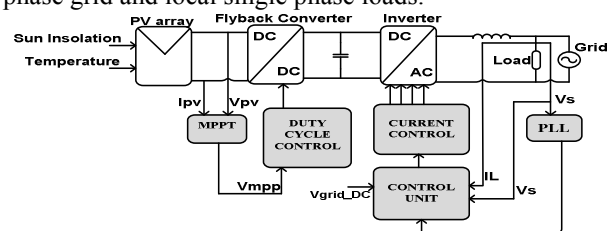


Fig. 1 The Overall system modelling including control signals.

As shown in Fig. 1, DC-DC converter is followed by an dc-ac (inverter). The converter is linked to the PV system with a filter capacitor C for reducing the high frequency ripple generated by the transistor switching. The dc-dc converter output is connected to the dc bus of the dc-ac converter as depicted in Fig. 2. The dc-dc converter produces a chopped output voltage and therefore controls the average dc voltage relation between its input and output aiming at continuously so the characteristic of the PV system and the dc-ac converter be matching.

The flyback boost DC/DC converter is made to drains the power from the PV solar cell array and supplies the DC link capacitor with a maximum power point tracker obtained from the MPPT controller. The steady-state voltage and current relations of the boost converter operating in continuous current mode are [4]:

$$V_D = \frac{V_{PV}}{1-D} \quad (1)$$

$$I_D = \eta_b(1-D)I_{PV} \quad (2)$$

where:

η_b : efficiency of the boost converter, D : dc-dc converter duty cycle, I_{pv} : PV array output current, V_{pv} : PV array output voltage, I_D : Dc bus current (inverter side) & V_D : Dc bus voltage (inverter side)

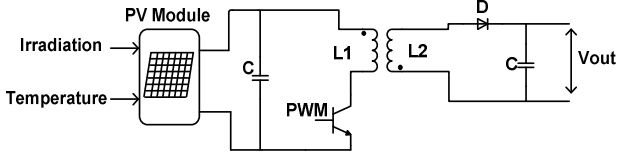


Fig. 2 Schematic of the boost dc-dc converter as a part of the grid-connected PV system.

The fly back transformer provides isolation and also the voltage ratios are multiplied by turn's ratio. Fly back transformer model includes an primary inductance L1 with value 300 uH, and an ideal transformer with a turn's ratio N_1/N_2 . The leakage inductance and losses of the Fly back transformer are neglected here [5]. But the leakage inductance affects the switch and diode transitions. The relation between output and input for voltage and current are:

$$V_o = V_g * \left(\frac{D}{1-D}\right) * \left(\frac{N_2}{N_1}\right) \quad (3)$$

$$I_g = I_o * \left(\frac{D}{1-D}\right) * \left(\frac{N_2}{N_1}\right) \quad (4)$$

III. MPPT ALGORITHM

In order to track the time varying maximum power point of the solar array depending on its operating conditions of insolation and temperature [6]. This paper propose an MPPT and compmers it with different MPPT control techniques. It is known that the output power of PV arrays varies with weather conditions. Therefore, real time MPPT control for extracting maximum power from the PV panel becomes indispensable in PV generation systems [7]-[8]. The MPPT techniques used are discussed below.

A. Conventional method (Incremental Conductance)

This method based on measuring the power of PV module (current and voltage). The maximum power point tracking (MPPT) algorithm that is used, is based on the differentiation of PV power and on condition of zero slope of PV curve [9]. Typical conventional system advantages are: Fast response for any change in temperature and irradiation, simple control and separate control for boost and inverter. The main disadvantages are: MPPT depends on power of PV module and needs more control signals.

B. Proposed Power Conditioning Method

The advantages of this scheme are low inverter current, reduced filter size, and small overall size. That can be seen because it doesn't need to measure the PV power to control the flyback converter but it uses the inverter power (output power) to control it. Using inverter power requires only measuring the inverter current or its corresponding signal. That reducing measuring devices. The conventional two-stage PCS is shown in Fig. 3. These approaches use the DC-link voltage error (see Fig. 7), which represent the inverter current variation, to control the duty of the flyback boost converter, which is proportional to the solar array output power for the MPPT.

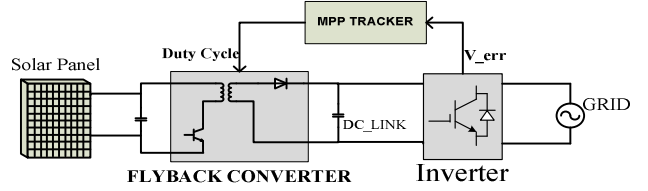


Fig. 3 Two-stage scheme of utility grid-connected PCS.

The benefits of this method it performs MPPT without the solar array power calculation. This simple operation principle offers cost competitiveness and compactness of size because it reduces the measured signals. The following assumptions for the MPPT control method in two-stage PCS schemes is considered: the DC-link voltage regulation control loop is much faster than the MPPT loop, and the efficiency of the boost is almost constant throughout the operating points. By maintaining the DC-link voltage constant, the output of the voltage loop, V_{err} , determines the output current amplitude, and thus controls the level of power processed by the PCS [10]- [11].

For the constant DC-link voltage, the input current of the inverter is directly proportional to the solar array output power. Thus, using V_{err} , the MPP can be tracked without calculating the solar array output power. Figure 4 shows the flowchart of the MPPT algorithm, and The complete system is shown in Fig. 7.

$$V_{err} = K_p(V_{dc_{link}} - V_{ref}) + \frac{K_I}{S}(V_{dc_{link}} - V_{ref}) \quad (5)$$

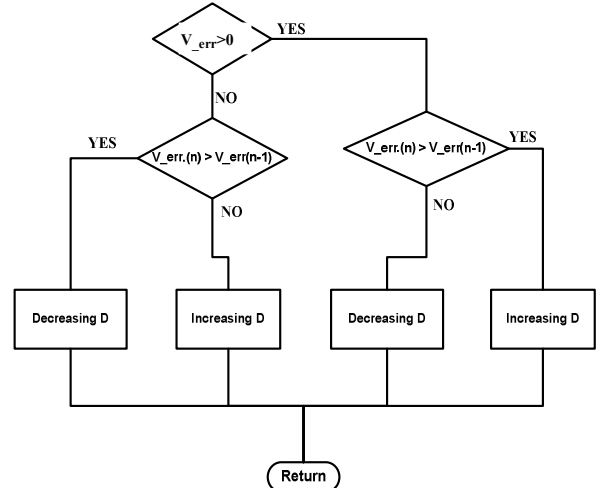


Fig. 4 The flowchart of the MPPT algorithm.

C. MPPT using Fuzzy Logic Control

As stated before, MPPT using Fuzzy Logic Control gains several advantages of better performance, reliability and simple design. In addition, this technique does not require the knowledge of the exact model of system and it can handle the nonlinearity. The main parts of FLC, fuzzification, rule-base, inference and defuzzification. The proposed FL MPPT controller has two inputs and one output [12]. The two FLC input variables are the error E and change of error CE at sampled times j defined by:

$$P_{PV} = V_{PV} * I_{PV} \quad (6)$$

$$E(j) = \frac{P_{PV}(j) - P_{PV}(j-1)}{V_{PV}(j) - V_{PV}(j-1)} \quad (7)$$

$$CE(j) = E(j) - E(j-1) \quad (8)$$

where P_{pv} , I_{pv} , V_{pv} are the PV power, current and voltage respectively at instant j . $E(j)$ shows if the load operating point at the instant j is located on the left or on the right of the maximum power point on the P-V characteristic where it is equals to zero at MPP. While the change of error $CE(j)$ expresses the moving direction of this point. Where the control action duty cycle D used for the tracking of the maximum power point by comparing with the saw tooth waveform to generate a PWM signal for the flyback boost converter [17]. In the defuzzification stage, the fuzzy logic controller output is converted from a linguistic variable to a numerical variable still using a membership function. This provides an analog signal that will control the power converter to the MPP [13]. In this paper Mamdani's fuzzy inference method, with Max-Min operation fuzzy combination has been used [14]-[15]. The membership functions for the variable are shown in Fig. 5.

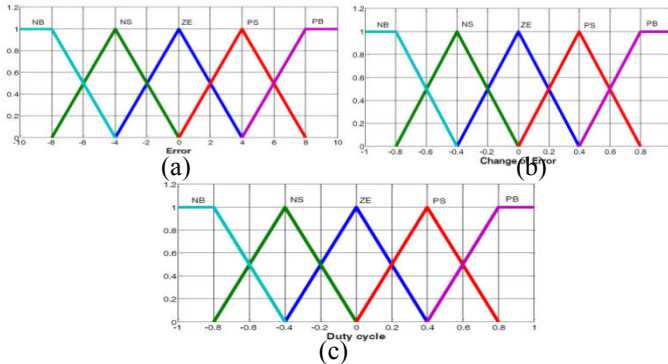


Fig.5. Membership function of (a) error E - (b) change of error CE - (c) duty ratio D .

Figure 6 shows the proposed system using FLC.

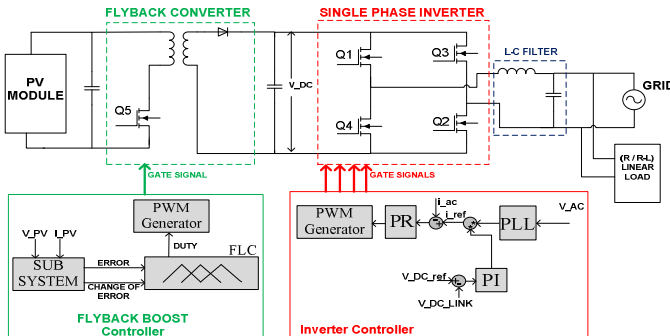


Fig. 6 Proposed system using FLC.

The control rules are indicated in Table I with E and CE as inputs and D as the output.

Table I: Fuzzy rules base

$CE \backslash E$	NB	NS	ZE	PS	PB
NB	ZE	ZE	PB	PB	PB
NS	ZE	ZE	PS	PS	PS
ZE	PS	ZE	ZE	ZE	NS
PS	NS	NS	NS	ZE	ZE
PB	NB	NB	NB	ZE	ZE

D. Power Conditioning Method using Fuzzy Logic Controller

In this method the FLC is used to determine the duty cycle for the flyback converter. The differ from the previous method is the inputs for FLC is V_{err} , which comes from the voltage loop in the inverter controller. This method gives faster response than PCS, and at the same time it doesn't need to know directly PV data. Moreover, it reduces the control signals used in the system. Figure 7 shows the proposed system.

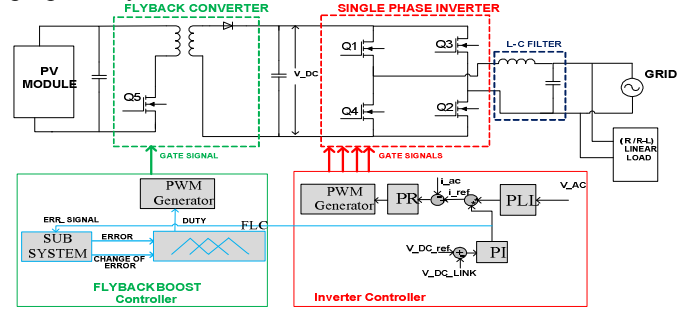


Fig. 7 Proposed system for PCS using FLC.

IV. INVERTER CONTROL LOOPS

The control objective of the grid-tied inverter is to output unit power factor sinusoidal current and maintain constant dc link voltage V_{dc} . The grid-tied inverter adopts two control loops, voltage loop and current loop. The PI controller is used to control the voltage V_{dc} , while the PR controller is adopted to control the current i_{ac} .

The electrical dynamics of the grid-tied inverter can be described as follows:

$$V_{DC} = L \frac{di_{ac}}{dt} + i_{ac}R + V_{ac} \quad (9)$$

The output current i_{ac} is desired to be a line frequency AC sinusoidal signal to achieve unity power factor. Resonant controller is an internal model principle based controller which can be used to track sinusoidal signal with zero steady-state tracking error. Therefore, a proportional-resonant (PR) controller is proposed to be the current controller as follows [16],

$$G_o(s) = \frac{Y(s)}{E(s)} = \frac{2K_r \omega_c s}{s^2 + 2\omega_c s + \omega^2} \quad (10)$$

The transfer function of PR can be represented in block diagram shown in Fig. 8.

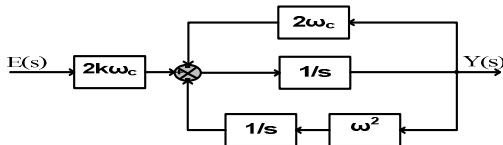


Fig. 8 implemented of PR controller.

The magnitude-frequency characteristic of the PR is described as:

$$|A| = \sqrt{K_p^2 + \frac{K_i^2 \omega_c^2}{-\omega^2 + \omega_0^2}} \quad (12)$$

Since A is infinite at $\omega = \omega_0$, zero steady-state errors tracking can be obtained at $\omega = \omega_0$. The inverter has the voltage loop to regulate the input DC-link voltage and the current loop to control the output current to be in-phase with the line voltage for a high power factor. After the dc-ac inverter an LC filter is inserted in order to eliminate the harmonics contained in both the voltage and current of the inverter output [17]. The main task of the grid connected PV system control system is to be sure that the signals of the inverter output and grid signals have the same frequency, phase and RMS values. Any deviation in these parameters PV system must be disconnected from the grid, sensors are used to sense the lines for any deviations in frequency and voltage and will disconnect the PV system from the grid when necessary [18].

V. SIMULATION RESULTS

In order to investigate the effectiveness of the proposed model and control algorithms of the signal phase grid connected PV system, a group of simulations results has been presented using Simulation Power Systems of MATLAB / Simulink environment.

The system parameters are listed in T II. And Fly-back transformer parameters are listed in Table III.

Table II: system parameters

Symbol	Quantity	Values
P_{MPPT}	Rated power	199 W
V_{MPPT}	Rated voltage	26.3 V
I_{MPPT}	Rated current	7.6 A
V_{OC}	Open-circuit voltage	32.9 V
I_{SC}	Short-circuit current	8.21 A
N_S	Number of series cell	54
N_P	Number of parallel cell	1
N_{Sm}	Number of series module	1
N_{Pm}	Number of parallel module	1
C	Solar capacitor	4700 μ F
T_C	Atmospheric Temperature	25°C
G_N	Solar Irradiation	1000 W/m ²
V_S	Grid voltage in RMS	220 V
V_{DC}	DC reference voltage	312V
C_{DC}	Fly-back capacitor	3.6mF
L_S	Grid tied inductor	30mH
C_F	DC-bus capacitor	5 μ F
F_{SM}	Sampling frequency	5kHz
F_{SW}	Switching frequency	5kHz
F	Line frequency	50Hz

Table III: Fly-back HF transformer parameters:

Quantity	Symbol	Values
Inductance	L_{boost}	28 μ H
DC resistance	DCR Primary	0.008 Ohms
DC resistance	DCR Secondary	0.472 Ohms
Self-Resonant Frequency	SRF	360 kHz
Saturation current	Isat.	10.5 A
Turns ratio	Pri:Sec	1:12

Figure 9 represent the typical conventional system (Inc. Cond.) at constant irradiation:

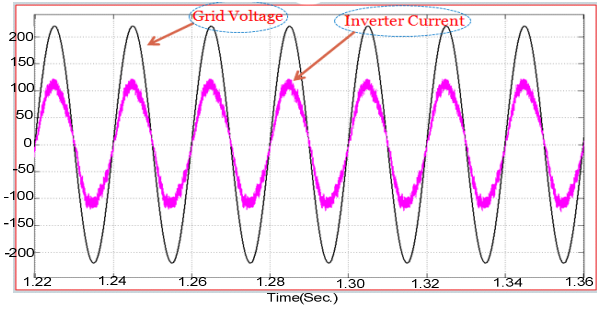


Fig.9 Relation bet. {I-inv., V-grid}.

Figures 10-11 show the difference between INC. COND. method, PCS and FLC in PV power and inverter power at variable weather conditions.

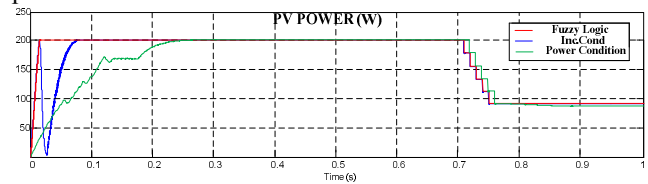


Fig. 10 PV power with different weather conditions in (incremental conductance, FLC and PCS)

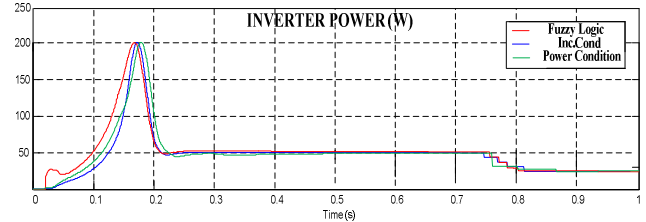


Fig. 11 inverter power with different weather conditions in (incremental conductance, FLC and PCS)

Figures 12-13 show the PV power and inverter power in case of FLC, PCS and PCS using FLC.

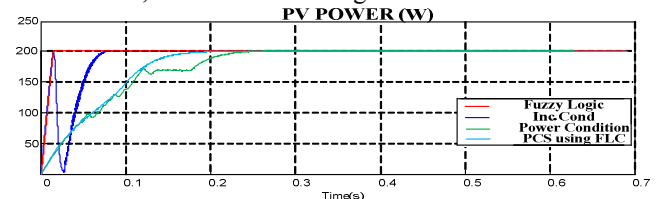


Fig. 12 PV power with different weather conditions in (incremental conductance, FLC, PCS and PCS using FLC)

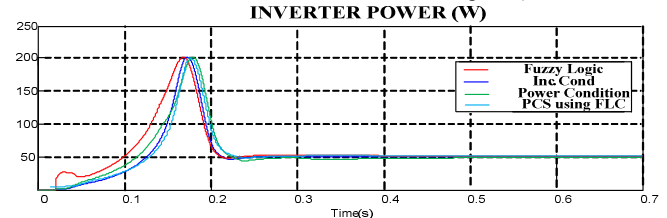


Fig. 13 Inverter power with different weather conditions in (FLC, PCS and PCS using FLC)

In order to check the robustness and sensitivity of the studied MPP techniques, variable environmental conditions are tested. Moreover, the load variation effect is studied.

A. Validation of active power generation

The system under test is modelled and simulated with 100W and 200W resistive loads then the resistive load increased to 400W and 1KW. The current simulation results for 100W and 200W loading conditions, presented in Fig. 14, show that the grid current is in phase with respect to the grid voltage, i.e. the inverter current supply the load and the grid according to $I_I = I_L + I_G$. It is seen in Fig. 15 from the current simulation results after the load increment to 400W and 1KW that the grid current is now out phase with respect to the grid voltage. This means that the inverter current and the grid are both supplying the load ($I_L = I_I + I_G$).

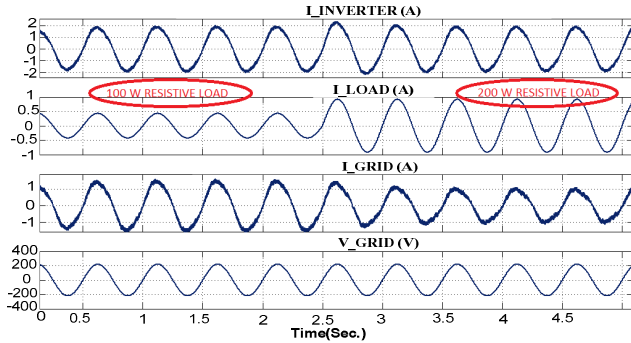


Fig. 14 Simulation Result for PV Inverter, Load and Grid currents with 100 W and 200W resistive linear loads.

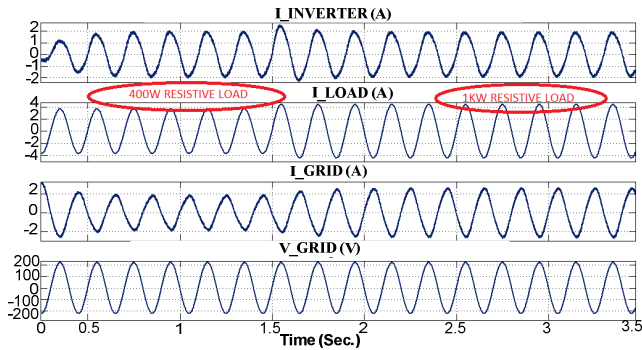


Fig. 15 Simulation Result for PV Inverter, Load and Grid currents with 400W and 1 kW resistive linear loads.

Figures 16-19 show the changes in PV current, PV voltage, DC link voltage, grid current and load current for the same load when the condition of irradiation and temperature are changes in case of fuzzy, incremental conductance, PCS and PCS using FLC control methods respectively.

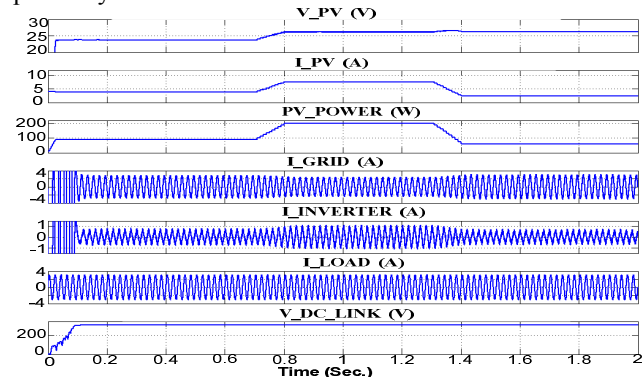


Fig. 16 Simulation Result for PV current, PV voltage, DC link voltage, grid current and load current with 900W loads with {fuzzy controller}.

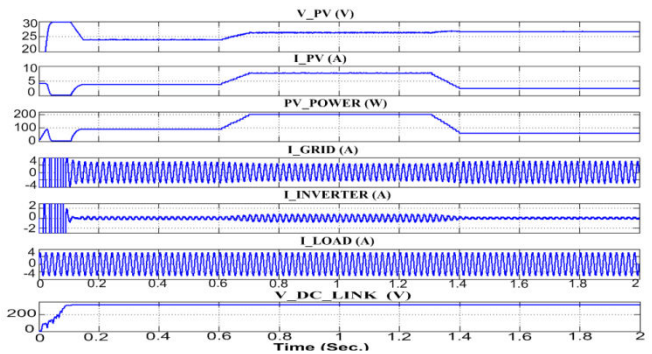


Fig. 17 Simulation Result for PV current, PV voltage, DC link voltage, grid current and load current with 900W loads with {incremental conductance control}.

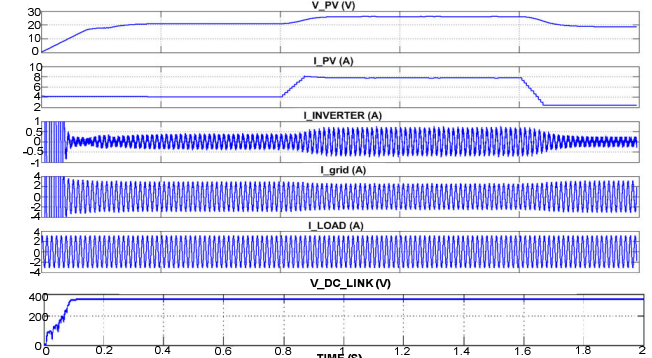


Fig. 18 Simulation Result for PV current, PV voltage, grid current and load current with 900W loads with {power conditioning system control}.

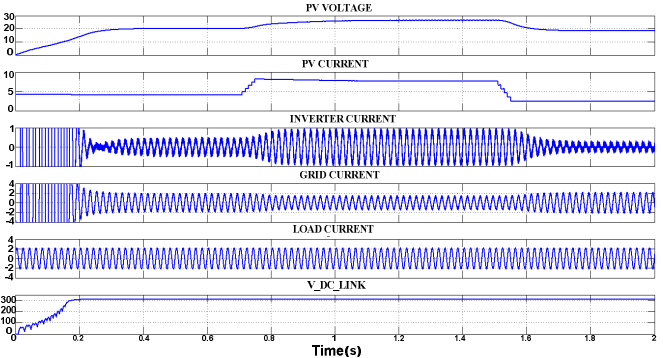


Fig. 19 Simulation Result for PV current, PV voltage, grid current and load current with 900W loads with {PCS using FLC}.

B. Validation of reactive power compensation

To emphasize the inverter capability to compensate for local reactive loads, the inverter has been operated with an R L load type. This simulation test has been performed with the inverter having a 100 W and 80Var load as shown in Fig. 20. At the first loading condition the simulated load current lags the load voltage by about 35° electrical degrees, while it can be noted that the grid current maintains to be pure active (in phase with grid voltage) since the inverter completely compensates for the load reactive power requirements. At the second load condition the load current lags the load voltage by about 35° electrical degrees and it can be seen that the grid current lagging with respect to the grid voltage by 180° electrical which means active power generation since the inverter generates more active power than the active power load requirements.

The results shows that FLC has the fastest respond for any change in weather conditions, but it use more control

signals than PCS. And for the incremental conductance method the control signals is the same with FLC but the response is slower. So for the applications needs fast response the FLC is recommended but the cost will increase, while for other applications PCS will be more recommended because it used less control signals and that means decrease cost. Combine FLC with PCS enhance the performance of PCS alone. Table IV shows the difference between MPPT control techniques at insolation = 1000 w/m² and temperature = 25C°.

At the same time the results show the effect of weather condition on the PV power and inverter power. Also, the effect on the load power, and the cases when the inverter feed the grid or absorb power from it.

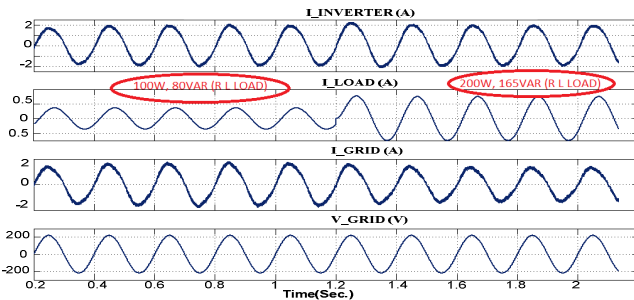


Fig. 20 Simulation Result for PV inverter, load current, grid current and grid voltage with 100W-80 VAR and 200W-165VAR inductive linear loads.

Table IV: Comparison between control techniques

Techniques	PV power (W)	Response Time (s)	Measurements signal
INCREMENTAL CONDUCTANCE	200.09	0.07	I_{pv} , V_{pv} , V_{dc} link, I_{grid}
FLC	199.95	0.02	I_{pv} , V_{pv} , V_{dc} link, I_{grid}
PCS	200.1	0.25	V_{dc} link, I_{grid}
PCS using FLC	199.5	0.15	V_{dc} link, I_{grid}

VI. CONCLUSIONS

In order to construct a PV grid connected system, a number of parameters have to be taking into account and to be optimized in order to achieve maximum power generation. The maximum power point tracking algorithm has applied using different control strategies (Fuzzy, Incremental Conductance, PCS and combined Fuzzy and PCS). In addition to that a controller has to be used in order to achieve the synchronization to the grid and to perform the power management between the system and the electrical grid.

Some points should be covered in the future such as: Practical implementation to verify the simulation results, the implementation of Multi Stage Grid Connected Photovoltaic System in case of three phase loads, study the non linear loads and Active Power Filter (APF) including its control methods.

REFERENCES

[1] T. Shimizu, O. Hashimoto, and G. Kimura, "A Novel High Performance Utility-Interactive Photovoltaic Inverter System." IEEE Trans. Power Electron, vol. 18, no. 2, pp. 704-711, Feb. 2003.

[2] P. D. Maycock, "World PV Cell/Module Production," PV News, vol. 25, no. 3, Mar. 2006.

[3] H. El-helw, M. Hassanien, H.A. Ashour, "Maximum power point tracking for irregular irradiance of a photovoltaic array", in Environment and Electrical Engineering (EEEIC), 12th International Conference on Wroclaw, Poland, pp. 52 – 57, 5-8 May 2013.

[4] E. Duran, J. Sidrach-de-Cardona, M. Galan and J.M.Andjar "Comparative Analysis of Buck-Boost Converters Used to Obtain I-V Characteristic Curves of Photovoltaic Modules", IEEE Power Electronics Specialists Conference, Rhodes, pp. 2036 – 2042, 15-19 June 2008.

[5] H.Sugimoto et al., "A New Scheme for Maximum Photovoltaic Power Tracking Control," in 1997 PCC-Nagaoka Proc., Nagaoka, Japan, Vol.2, pp.691-696, 3-6 Aug 1997.

[6] M. Matsui et al. , "New MPPT Control Scheme Utilizing Power Balance at DC Link Instead of Array Power Detection," in 2000 IEEE IPEC-Tokyo Proc., Tokyo, Japan, Vol.1, pp. 164-169, 2000.

[7] Trishan Efram, Patrick L. Chapman, "Comparison of Photovoltaic Array Maximum Power Point Tracking Techniques," IEEE Trans. on Energy Conversion, Vol.22, no.2, pp.439-449, June 2007.

[8] G.M.S. Azevedo, M.C. Cavalcanti, and K.C. Oliveira, "Evaluation of Maximum Power Point Tracking Methods for Grid Connected Photovoltaic Systems," IEEE Power Electronics Specialists Conference, pp: 1456-1462, June, 2008.

[9] L. Fangrui, D. Shanxu, L. Fei, and L. Bangyin, "A Variable Step Size INC MPPT Method for PV Systems," IEEE Transactions on industrial Electronics, Vol.55, no.7, pp: 3622-3628, July, 2008.

[10] E. Trishan, and L. Chapman Patrick, "Comparison of Photovoltaic Array Maximum Power Point Tracking Techniques," IEEE Trans. on Energy Conversion, Vol.22, no.2, pp.439-449, June 2007.

[11] H. S. Bae, J. H. Park and B. H. Cho "New Control Strategy for 2-stage Utility-Connected Photovoltaic Power Conditioning System with a low cost digital processor", Electronics Specialists Conference, PESC '05. IEEE 36th, pp.7803-9033, 2005.

[12] H.E.A. Ibrahim, and M. Ibrahim, " Comparison Between Fuzzy and P&O Control for MPPT for Photovoltaic System Using Boost Converter", Journal of Energy Technologies and Policy, Vol.2, no.6, pp. 2224-3232, 2012.

[13] P. Aurobinda, M. K. Pathak, and S. P. Srivastava, "Fuzzy Intelligent Controller for The Maximum Power Point Tracking of a Photovoltaic Module at Varying Atmospheric Conditions", Journal of Energy Technologies and Policy, vol.1, no.2, pp.18-27, 2011

[14] M. Ajaamoum, M. Kourchi, R. Alaoui, and L. Bouhouch, "Fuzzy controller to extract the maximum power of a photovoltaic system", in Renewable and Sustainable Energy Conference (IRSEC), Ouarzazate, Morocco, pp. 141 – 146, 7-9 March 2013.

[15] B. Alajmi, K. Ahmed, G. Adam, and B. Williams, "Single Phase Single Stage Transformer less Grid Connected PV System" in IEEE Transactions on Power Electronics, Vol. 28, No. 6, pp. 2664-2676, June 2013.

[16] J. Mahdavi, A. Emadi, and H.A. Toliyat, "Application of State Space Averaging Method to Sliding Mode Control of PWM DC DC Converters," IEEE Industry Applications Society Annual Meeting, pp.820-827, October, 1997.

[17] M. G. Molina, and P. E. Mercado "Modeling and Control of Grid-connected PV Energy Conversion System used as a Dispersed Generator". Transmission and Distribution Conference and Exposition: IEEE/PES, pp.4244-2218, 2008.

[18] M. P. Kazmierkowski, and M. A. Dzieniakowski, "Review of Current Regulation Methods for VS-PWM Inverters", Conference Proceedings, ISIE'96, Budapest, Hungary, IEEE International Symposium On, pp. 488-456, 1993.